Journal of Power Sources 196 (2011) 3104–3108

Contents lists available at ScienceDirect

Journal of Power Sources

journal homepage: www.elsevier.com/locate/jpowsour

Short communication

Preparation and electrochemical performance of $Pr_2Ni_{0.6}Cu_{0.4}O_4$ cathode materials for intermediate-temperature solid oxide fuel cells

Yifang Wang[a], Jigui Cheng[a,*], Qiumei Jiang[a], Junfang Yang[a], Jianfeng Gao[b]

[a] School of Materials Science and Engineering, Hefei University of Technology, Hefei, Anhui 230009, PR China
[b] Department of Materials Science and Engineering, University of Science and Technology of China, Hefei, Anhui 230026, PR China

ARTICLE INFO

Article history:
Received 9 September 2010
Received in revised form 9 November 2010
Accepted 22 November 2010
Available online 30 November 2010

Keywords:
Solid oxide fuel cell
Cathode materials
Glycine–nitrate process
Electrochemical performance

ABSTRACT

Cathode material $Pr_2Ni_{0.6}Cu_{0.4}O_4$ (PNCO) for intermediate-temperature solid oxide fuel cells (IT-SOFCs) is synthesized by a glycine–nitrate process using Pr_6O_{11}, NiO, and CuO powders as raw materials. X-ray diffraction analysis reveals that nanosized $Pr_2Ni_{0.6}Cu_{0.4}O_4$ powders with K_2NiF_4-type structure can be obtained from calcining the precursors at 1000 °C for 3 h. Scanning electron microscopy shows that the sintered PNCO samples have porous microstructure with a porosity of more than 30% and grain size smaller than 2 μm. A maximum conductivity of 130 S cm^{-1} is obtained from the PNCO samples sintered at 1050 °C. A single fuel cell based on the PNCO cathode with 30 μm $Sm_{0.2}Ce_{0.8}O_{1.9}$ (SCO) electrolyte film and a 1 mm NiO–SCO anode support is constructed. The ohmic resistance of the single Ni–SCO/SCO/PNCO cell is 0.08 Ω cm^2 and the area specific resistance (ASR) value is 0.19 Ω cm^2 at 800 °C. Cell performance was also tested using humidified hydrogen (3% H_2O) as fuel and air as oxidant. The single cell shows an open circuit voltage of 0.82 V and 0.75 V at 700 °C and 800 °C, respectively. Maximum power density is 238 mW cm^{-2} and 308 mW cm^{-2} at 700 °C and 800 °C, respectively. The preliminary tests have shown that $Pr_2Ni_{1-x}Cu_xO_4$materials can be a good candidate for cathode materials of IT-SOFCs.

1. Introduction

Solid oxide fuel cell has been considered as one of the most promising energy conversion devices due to their high energy conversion efficiency, less emission of pollutants and flexibility of fuels [1,2]. In particular, the possibility of direct utilization of hydrocarbon and renewable fuels (e.g., methane and ethanol) will greatly reduce the cost of SOFC technology [3]. A conventional SOFC generally operates at high temperature (>800 °C), which not only leads to complex material degradation and reaction, but also limits material choice of the cell components [4]. Therefore, much work has been done to reduce the operating temperature of SOFC to low to intermediate temperature range (600–800 °C). However, as the operating temperature decreases, the cathode overpotential and interfacial resistances between the electrolyte and electrodes, especially cathode, also increase, leading to lower cell performance [5]. There are two ways to solve this problem. One is to use composite cathode materials to increase the areas of the triple phase boundary (TPB). Another is to find new mixed oxygen ionic and electronic conducting (MIEC) materials, which have rapid surface exchange kinetics, high oxygen vacancy concentration, and extended TPB from the gas/electrode/electrolyte interface to the total external electrode surface area [6,7].

Recently, A_2MO_4 oxides have received considerable attention in using as cathode materials for solid oxide fuel cells due to their interesting mixed transport properties [8]. The A_2MO_4 oxides, with M a transition metal cation like Ni and A, a lanthanide or alkaline earth, characterizes some oxygen over stoichiometry and a mixed valence of M in the compound [6]. The crystal structure of A_2MO_4 oxides can be described as taking of perovskite layers alternating with NaCl (rock salt) layers. For a mixed oxygen–ionic and electronic conductor (MIEC) as the A_2MO_4 oxide, the change of composition or oxidation–reduction treatments can greatly affect the transport properties, and the cathode reaction $O_2 + 4e^- = 2O_2^-$ occurs at the gas–MIEC two-phase interface, whereas it takes place only at a triple-phase boundary if the cathode is a pure electronic conductor [8,9]. In this way, several systems have been proposed either by doping at the A position with alkaline-earths and with other rare earths like Nd or Pr or by doping in the M position with other transition metals, typically Cu and Co, leading to dramatic changes of the structural and physical properties. Ishihara et al. reported that among different rare earth cations at the A-site, those incorporated Pr^{3+} exhibit the highest electrical conductivity and the lowest overpotential values [10,11]. Therefore, a combination of Pr for A-site and Cu for M-site material $Pr_2Ni_{1-x}Cu_xO_4$ is expected to bring better electrochemical properties as a cathode material at intermediate temperature. Aguadero et al. investigated the electro-

* Corresponding author. Tel.: +86 551 2901793; fax: +86 551 2901793.
E-mail address: jgcheng63@sina.com (J. Cheng).

0378-7753/$ – see front matter © 2010 Elsevier B.V. All rights reserved.
doi:10.1016/j.jpowsour.2010.11.106

chemical property of $La_2Ni_{1-x}Cu_xO_4$ materials and reported that among the $La_2Ni_{1-x}Cu_xO_4$ (x = 0–1.0) system, the $La_2Ni_{0.6}Cu_{0.4}O_4$ composition exhibits the highest electrical conductivity [8].

In this paper, $Pr_2Ni_{0.6}Cu_{0.4}O_4$ (PNCO) powders were synthesized by a glycine–nitrate methods. The microstructure and electrochemical property of the sintered PNCO material, including the electrical conductivity, the ohmic resistance and the electrode interfacial resistance were investigated, and single cells based on the PNCO cathode were also constructed and tested [12].

2. Experimental

2.1. Sample preparation

$Pr_2Ni_{0.6}Cu_{0.4}O_4$ powder was prepared by a glycine nitrate method using Pr_6O_{11} (AR), NiO (AR), CuO (AR) powders, HNO_3 (AR) and $C_2H_5NO_2$ (AR) as raw materials. Stoichiometry chemicals were dissolved into nitric acid to get a nitrate solution. Then glycine was added into the solution to form a transparent and homogeneous solution, which was subsequently heated and the viscosity of the solution increases gradually [13]. As temperature rises, a self-sustaining combustion finally occurs in the viscous gels and dark precursor powders were obtained. The precursor powders were then calcined at 1000 °C for 3 h to remove residue organics and form a stable crystalline structure. The calcined powders were subsequently pressed in a rigid die, and the compacts were then sintered at 900–1050 °C for 2 h for later test.

Commercial NiO (2.5 μm) and $Sm_{0.2}Ce_{0.8}O_{1.9}$ (SCO, prepared by the gel-casting process, 30 nm) powders were employed to prepare the NiO/SCO anode substrates. After mechanically blending (NiO:SCO = 60:40 wt%), the powder mixes were compacted in a steel die with 18 mm in diameter, the green anode substrates were fired at 1000 °C for 2 h. SCO electrolyte slurry was prepared onto the fired NiO/SDC substrates by a dip-coating method. The coated samples were then co-sintered at 1400 °C for 4 h to obtain anode/electrolyte bilayer structure with dense SCO electrolyte film supported on porous NiO/SCO substrates. After screen-printing $Pr_2Ni_{0.6}Cu_{0.4}O_4$ slurry onto the electrolyte side of the NiO/SCO bilayer and subsequently sintering at 1050 °C for 2 h, single cells were obtained [14]. The active area of the cathode in the single cells was 0.24 cm^2. Thickness of the anode, the cathode and the electrolyte in the single cell is about 1 mm, 100 μm and 30 μm, respectively.

2.2. Sample characterization

Phase structure of the precursors and the calcined $Pr_2Ni_{0.6}Cu_{0.4}O_4$ powders were characterized by X-ray diffraction analysis (XRD). Porosity of the PNCO samples sintered at different temperatures was tested using the Archimedes method with a theoretical density of $Pr_2Ni_{0.6}Cu_{0.4}O_4$ taken as 7.38 g cm^{-3}, which was calculated according data obtained from the XRD pattern. Microstructure of the PNCO samples sintered at different temperature was observed by scanning electron microscope (SEM, Sirion 200). Electrical conductivity of the sintered PNCO samples was measured using the four-probe method. Single cell performance was tested using a house-made fuel cell testing device, with humidified hydrogen (3% H_2O) as the fuel and steady air as the oxidant. Impendence spectra of the single cells were also tested using an electrochemical workstation (Chenhua 604A) under open-circuit conditions over a frequency range from 0.01 Hz to 1 MHz, with signal amplitude of 10 mV. The spectra were simulated by the Zsimpwin software.

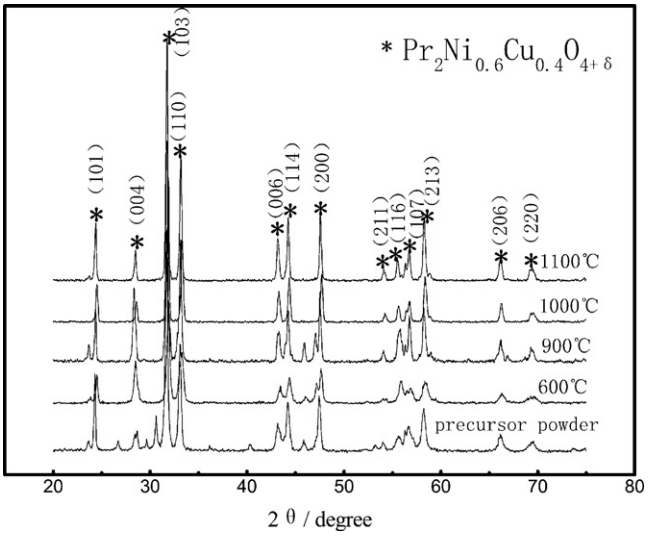

Fig. 1. XRD patterns of the PNCO powders calcined at different temperature.

3. Results and discussions

3.1. XRD analysis

Fig. 1 shows XRD patterns of the precursors and the calcined $Pr_2Ni_{0.6}Cu_{0.4}O_4$ powders. There exist some peaks of miscellaneous phases in the XRD patterns of the precursor powders. This indicates that the chemicals did not react completely during the self-sustaining combustion. It can be seen from Fig. 1 that as the calcining temperature increases, miscellaneous phases reduce. And when calcining temperature increases to 1000 °C, only K_2NiF_4-type structure was observed in the XRD patterns. The samples retained the K_2NiF_4-type structure when the calcining temperature increases to 1100 °C. But the diffraction peaks become sharper and narrower than those of 1000 °C, which indicates grain growth of the calcined powders.

According to the crystalline structure and the molecular formula of the PNCO powders, the grain parameters were calculated. The lattice content values are a = 5.456, b = 5.392, c = 12.446, α = 90°, β = 90°, γ = 90°. The grain size of the PNCO powders calcined at 1000 °C is 29.02 nm based on the Scherrer Formula. And the theoretical density of the PNCO powders is calculated to be 7.38 g cm^{-3}.

3.2. Porosity and microstructure of the sintered PNCO samples

Table 1 lists relative density and open porosity of the $Pr_2Ni_{0.6}Cu_{0.4}O_4$ samples sintered at different temperature. As sintering temperature increases, the samples become dense. While the samples sintered at 900 °C have an open porosity of 51%, the samples sintered at 1100 °C only have an open porosity of 27%. Fig. 2 shows SEM microstructure of the PNCO samples sintered at different temperature. All of the sintered samples have porous structure. This porous structure can facilitate the diffusion of oxidant gases and extend the area of the triple-phase boundary (TPB). However, as the sintering temperature increases, the porosity of the PNCO samples deceases. This is consistent with the results listed in Table 1.

Table 1
Open porosity and relative density of the PNCO samples sintered at different temperature.

Sintered temperature (°C)	900	1000	1050	1100
Open porosity (%)	51.10	44.13	37.24	27.12
Relative density (%)	45.12	53.38	59.33	66.50

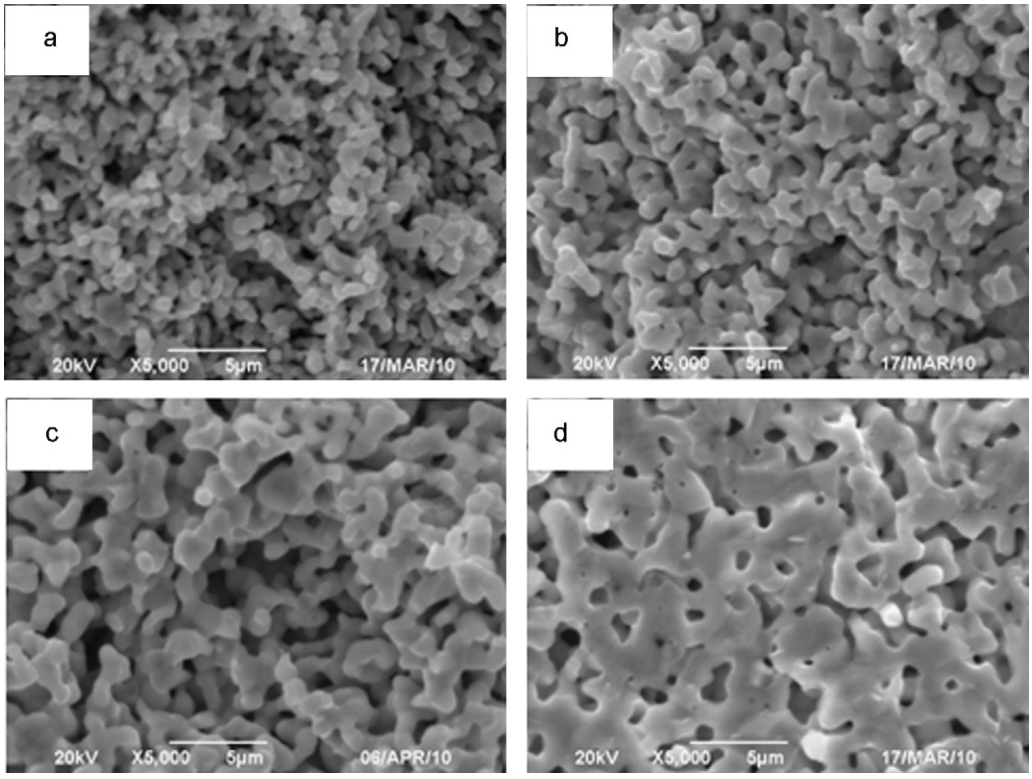

Fig. 2. SEM images of the as-prepared PNCO samples sintered at: (a) 900 °C; (b) 1000 °C; (c) 1050 °C; (d) 1100 °C.

It can also be seen from Fig. 2 that the samples sintered at lower temperature have a smaller grain size. Average grain sizes of the PNCO samples sintered at 900 °C, 1000 °C, 1050 °C and 1100 °C is about 0.7, 0.8, 1.0 and 1.5 μm, respectively.

3.3. Electrical conductivity

Electrical conductivity (σ) of the sintered $Pr_2Ni_{0.6}Cu_{0.4}O_4$ samples was measured in air by the four-probe method in the temperature range from 500 to 800 °C. Fig. 3 shows electrical conductivity as a function of testing temperature of the PNCO samples. As the sintering temperature of the PNCO samples increases, electrical conductivity increases gradually. A maximum conductivity of 130 S cm^{-1} was got for samples sintered at 1050 °C under testing temperature 500 °C. As sintering temperature increases, the samples become dense and the grain grows, which are beneficial to the transfer of ions and electrons, thus leading to the increase of electrical conduction. However, when the sintering temperature increases to 1100 °C, the conductivity of the sample becomes lower than that sintered at 1050 °C. This may be caused by the loss of surface area of grain boundaries, which results from the grain growth as sintering temperature. It can also be seen from Fig. 3 that conductivity of the PNCO samples decreases as measuring temperature increases, which indicates the electron conduction of the PNCO materials.

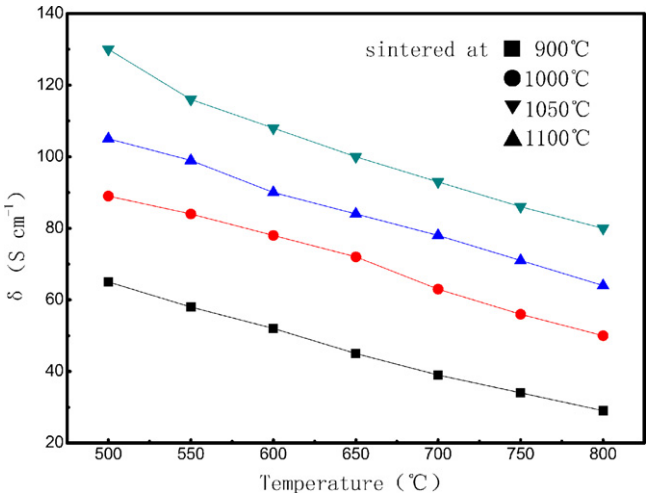

Fig. 3. Electrical conductivity of the sintered PNCO samples as a function of testing temperature.

Boehm et al. reported that $La_2Ni_{0.6}Cu_{0.4}O_4$ material with K_2NiF_4-type structure has a conductivity of 87 S cm^{-1} at 580 °C [6]. This value is lower than the conductivity value of $Pr_2Ni_{0.6}Cu_{0.4}O_{4+\delta}$ obtained in this work (about 130 S cm^{-1}). This may be caused by the different ionic of La^{3+} (1.06 Å) with Pr^{3+} (1.01 Å) and the additional contribution of the Pr^{3+}/Pr^{4+} valence change [11]. Average conduction activation energy was calculated from the $\ln\sigma$ and T^{-1} values, and the result is about 0.189, 0.137,0.110 and 0.114 eV for PNCO samples sintered at 900 °C, 1000 °C 1050 °C and 1100 °C for 2 h, respectively. The low-temperature sintered samples show slightly high resistant potential. This is consistent with the ionic conduction values.

3.4. Impedance spectra results

Fig. 4 shows impedance spectra of the NiO–SCO/SCO/PNCO single cell at 800 °C in air. The high-frequency intercept with the real axis represents the ohmic losses, and the difference between the high frequency and low frequency intercepts denotes the total electrode interfacial resistances in the cell. The ASR value obtained in this work is the total electrode resistance. It includes the contribution of the anode and the cathode. Min Chen et al. have reported the ASR values of Ni/SDC electrodes [15], which is about 0.12 Ω cm^2

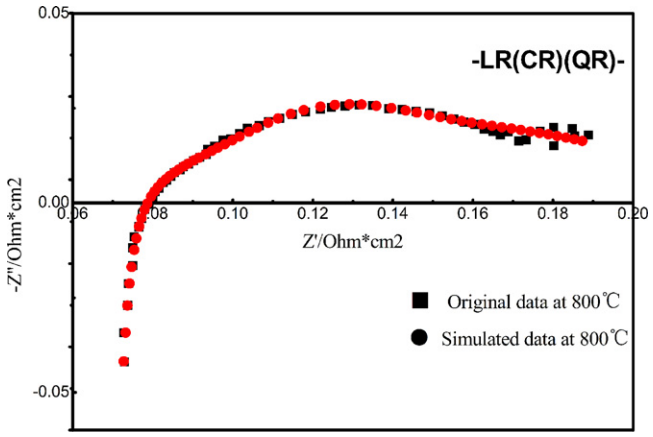

Fig. 4. AC impendence spectra of the single NiO–SCO/SCO/PNCO cell.

for a Ni/SDC anode with 60% NiO. In this work we simply use this value as the anode ASR of the single cell we prepared, and because the total ASR value of the single cell tested is 0.19 Ω cm^2, the cathode ASR value was calculated to be about 0.07 Ω cm^2. It has been reported that the ASR value of the $La_{0.6}Sr_{0.4}Co_{0.2}Fe_{0.8}$ O_3 material is about 0.30 Ω cm^2 [16]. By comparison, ASR value of the PNCO material is much lower. The lower ASR value of the PNCO material makes it have high-electrocatalytic activity for oxygen-reduction reactions at intermediate temperatures. The excellent cathodic performance of the PNCO material can be ascribed to the fast oxygen diffusion in the bulk and the high surface kinetics on the surface of electrode. Moreover, as a MIEC oxide, PNCO provides multiple pathways for the oxygen ions to migrate to the electrode/electrolyte interface.

3.5. Single cell performance

Fig. 5 shows the open circuit voltage (OCV) and power densities of a single solid oxide fuel cell with humidified hydrogen (3% H_2O) as fuel and air as the oxidant in the temperature range of 500–800 °C. The single cell shows a maximum open circuit voltage of 0.82 V and 0.75 V at 700 °C and 800 °C, respectively. However, with increasing testing temperature, the OCV value deceases and is lower than the theoretical values. This may be due to the electronic penetration through SCO electrolyte. Maximum power densities of the cell were 238 and 308 mW cm^{-2}

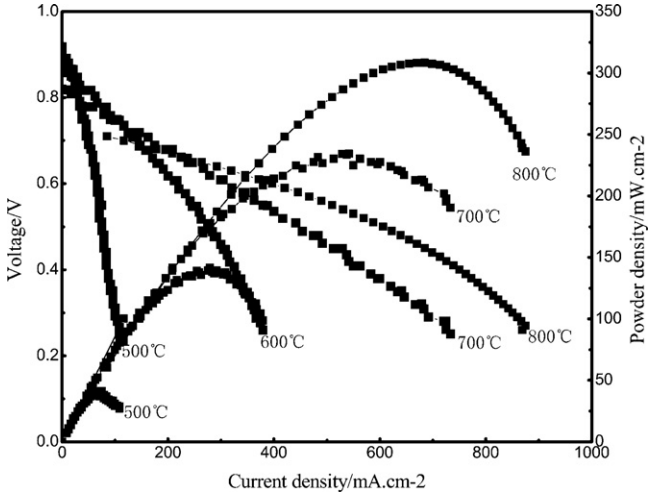

Fig. 5. I–V–P curves of the single NiO–SCO/SCO/PNCO cell at different test temperature.

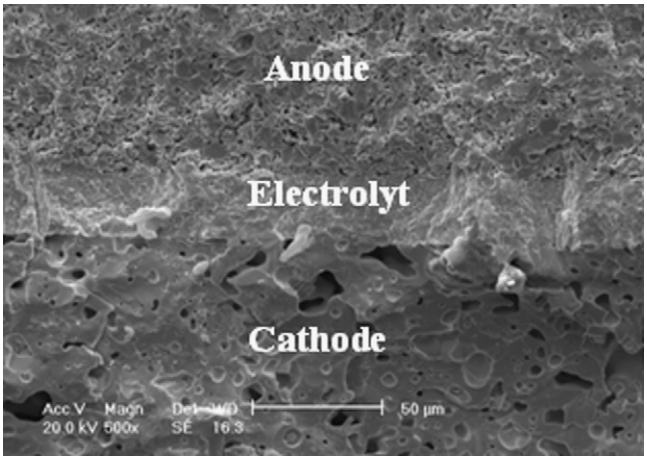

Fig. 6. Cross-section images of the single cell based on the PNCO cathode after test.

at 700 °C and 800 °C, respectively, indicating that good performance can be obtained for the single fuel cell using $Pr_2Ni_{0.6}Cu_{0.4}O_4$ as cathode and SCO film as electrolyte. It has mentioned above that the ASR value of $Pr_2Ni_{0.6}Cu_{0.4}O_4$ is lower than that of the $La_{0.6}Sr_{0.4}Co_{0.2}Fe_{0.8}O_3$ material. Therefore, the cell based on $Pr_2Ni_{0.6}Cu_{0.4}O_4$ cathode shows a better performance than the traditional cathode $La_{0.6}Sr_{0.4}Co_{0.2}Fe_{0.8}O_3$ [15]. Fig. 6 shows cross-section microstructure of the single cell after testing. There exists a good combination between the electrodes and the electrolyte.

4. Conclusions

$Pr_2Ni_{0.6}Cu_{0.4}O_4$ (PNCO) powders with K_2NiF_4-type structure were successfully synthesized by a glycine–nitrate method. Sintered PNCO samples have porous structure and good electrical conductivity. A maximum electrical conductivity of 130 S cm^{-1} was obtained at 500 °C in air. There exist low ohmic resistance and electrode interfacial resistance of 0.08 Ω cm^2 and 0.19 Ω cm^2, respectively. A single fuel cell based on the PNCO cathode with a 30 μm $Sm_{0.2}Ce_{0.8}O_{1.9}$ electrolyte and a 1 mm thickness NiO–SCO anode was constructed. The single cell shows an open circuit voltage of 0.82 V and 0.75 V and maximum power density of 238 mW cm^{-2} and 308 mW cm^{-2} at 700 °C and 800 °C, respectively. The present work has shown that the PNCO materials may be a favorable candidate for cathode material of intermediate temperature solid oxide fuel cells.

Acknowledgements

This work was financially supported by the Natural Science Foundation of Anhui Province (contract No. 070414186), the Program of Science and Technology of Anhui Province (contract No. 2008AKKG0332), the Nippon Sheet Glass Foundation for Materials Science and Engineering (NSCF) (contract No. 070304B2) and the Open Project Program of Key Laboratory of Low Dimensinal Materials & Application Technology (Xiangtan University), Ministry of Education of China under contract No. DWKF0802.

References

[1] P. Bansal Narottam, Z.M. Zhong, J. Power Sources 158 (2006) 148–153.
[2] C. Cacciola, V. Antonucci, S. Freni, J. Power Sources 100 (2001) 67–79.
[3] S.P. Jiang, Y.M. Ye, T.M. He, S.B. Ho, J. Power Sources 185 (2006) 1.
[4] S. Yang, T.M. He, Q. He, J. Alloys Compd. 450 (2008) 400–404.
[5] Q.J. Zhou, T.M. He, Q. He, Y. Ji, Electrochem. Commun. 11 (2009) 80–83.
[6] H. Zhao, F. Mauvy, C. Lalanne, J.M. Bassat, S. Fourcad, J.C. Grenier, Solid State Ionics 179 (2008) 35–36.

[7] H.A. Hamedani, K.H. Dahmen, D. Li, H. Peydaye-Saheli, H. Garmestani, M. Khaleel, Mater. Sci. Eng. B: Adv. Funct. Solid-State Mater. 153 (2008) 1–3.
[8] A. Aguadero, J.A. Alonso, M.J. Escudero, L. Dazaet, Solid State Ionics 179 (2008) 11–12.
[9] J. Wan, J.B. Goodenough, J.H. Zhu, Solid State Ionics 178 (2007) 281–286.
[10] C.J. Zhu, X.M. Liu, D. Xu, D.T. Yan, D.Y. Wang, W.H. Su, Solid State Ionics 179 (2008) 1470–1473.
[11] T. Ishihara, T. Kudo, H. Matsuda, Y. Takita, J. Electrochem. Soc. 142 (1995) 1519–1523.
[12] Y. Tao, H. Nishino, S. Ashidate, H. Kokubo, M. Watanabe, H. Uchida, Electrochim. Acta 54 (2009) 3309–3315.
[13] B. Yu, W.Q. Zhang, J.M. Xu, J. Chen, Int. J. Hydrogen Energy 33 (2008) 6873–6877.
[14] Tietz, F. Haanappel, V.A.C. Mai, A. Mertens, J. Stover, J. Power Sources 156 (2006) 20–22.
[15] J.D. Zhang, Y. Ji, H.B. Gao, T.M. He, J. Liu, J. Alloys Compd. 395 (2009) 322.
[16] E.P. Murray, M.J. Sever, S.A. Barnett, Solid State Ionics 148 (2002) 27–34.